

# Periodic orbit theory for realistic cluster potentials: The leptodermous expansion

Erik Koch

Max-Planck-Institut für Festkörperforschung, D-70569 Stuttgart

(November 13, 2017)

The formation of supershells observed in large metal clusters can be qualitatively understood from a periodic-orbit-expansion for a spherical cavity. To describe the changes in the supershell structure for different materials, one has, however, to go beyond that simple model. We show how periodic-orbit-expansions for realistic cluster potentials can be derived by expanding *only* the classical radial action around the limiting case of a spherical potential well. We give analytical results for the leptodermous expansion of Woods-Saxon potentials and show that it describes the shift of the supershells as the surface of a cluster potential gets softer. As a byproduct of our work, we find that the electronic shell and supershell structure is not affected by a lattice contraction, which might be present in small clusters.

71.24.+q, 71.20.-b, 31.15.Gy

## I. INTRODUCTION

One of the most surprising aspects of the physics of metal clusters is the supershell structure observed in mass-abundance spectra.<sup>1-4</sup> This feature can be traced back to a beating pattern in the density of states for typical cluster potentials.<sup>5</sup> The conceptual framework for understanding how this quantum interference comes about is provided by periodic-orbit-theory.<sup>6,7</sup> The elegance of this approach rests on the fact that the periodic-orbit-expansion (POE) is known analytically for the spherical cavity. For this model potential it was found that the most important contributions to the oscillating part of the density of states stem from the two shortest planar periodic orbits: the triangular and the square orbits. Since these contributions oscillate with similar frequencies, their interference gives rise to a beating pattern, hence supershells.

Although a spherical potential well is a good first approximation to a cluster potential, this model clearly cannot account for the changes in the electronic shell and supershell structure observed for clusters made of different materials. It is therefore desirable to understand how the periodic-orbit-expansion is modified as one considers more realistic model potentials. A straightforward approach for doing so is to solve the action integrals, which lie at the heart of periodic-orbit-theory, numerically. That way, however, most of the elegance and power of the periodic-orbit-expansion is lost. Analytical expression, on the other hand, may well reveal the relevant parameters determining the supershell structure, and provide insight into how it changes as the cluster potential is varied. They should prove especially helpful in the search for better self-consistent models, which properly describe the experimental data.

While the simple spherical, homogeneous jellium model<sup>8,9</sup> works quite well for the alkali clusters, it fails to describe the supershell structure observed in  $\text{Ga}_N$ .<sup>4</sup>

Attempts to improve the situation include, e.g. the introduction of smooth jellium-profiles,<sup>10</sup> the inclusion of pseudopotentials,<sup>11-13</sup> or the consideration of surface roughness.<sup>14</sup>

The present work arises from the desire to understand the simple spherical, homogeneous jellium model. An analysis of the density dependence of the electronic supershells in jellium clusters showed that the supershells are shifted as the potential at the cluster surface becomes softer.<sup>15</sup> It has been demonstrated that this shift can be understood in the framework of a periodic-orbit-expansion for typical self-consistent cluster potentials.<sup>16</sup> The purpose of the present paper is to give a derivation of the leptodermous expansion, which requires the linearization of *only the radial action*. We furthermore analyze the validity of the approximations involved and show comparisons with quantum mechanical calculations.

To set the stage for the semiclassical treatment of electronic supershells, Sec. II gives a review of the shell correction methods.<sup>17-19</sup> These methods establish a systematic relation between self-consistent calculations and one-electron calculations for suitable model potentials. We stress the fact that it is decisive to choose families of potentials that vary smoothly with cluster size, to describe the electronic shell structure properly.

Sec. III is devoted to periodic-orbit-expansions. We sketch the derivation of the POE for the oscillating part  $\tilde{\rho}$  of the density of states using the path integral formalism along the lines given by Gutzwiller.<sup>7</sup> Special attention is paid to the rate of convergence of the sum over classical periodic orbits. Since the shell and supershell structure observed in the mass spectra of metal clusters is not directly linked to  $\tilde{\rho}$  but rather the variations  $\tilde{E}$  in *total energy*, we proceed to derive a periodic-orbit-expansion for  $\tilde{E}$ . We find that the latter expansion converges much more rapidly than that for the density of states, hence making any artificial smoothing of the spectrum, commonly introduced to lessen the contribution of the longer

orbits to  $\tilde{\rho}$ ,<sup>6,5,20</sup> superfluous. To assess the validity of the expression for  $\tilde{E}$  we check the truncated POE against the quantum-mechanical result. This comparison shows that in the size range, which seems experimentally accessible,  $\tilde{E}$  is well described by a truncated POE, taking only triangular and square orbits into account. This justifies the common practice of truncating the POE after the two shortest *planar* orbits.

As an immediate application of the periodic-orbit-expansion for  $\tilde{E}$  we show in Sec. IV that the electronic shell structure is virtually not affected by any lattice contraction. Such an increase in density for small clusters was suggested by EXAFS analyses<sup>21,22</sup> and seems also plausible from the viewpoint of continuum mechanics, which implies that the surface tension should lead to a compression of the smaller clusters. We show that the major effect of a lattice contraction on  $\tilde{E}$  is a change of the amplitude for small clusters. The position of the shell minima and the supershell structure is, however, not noticeably changed, even for unrealistically large contractions.

In Sec. V we show how to extend the periodic-orbit-expansion of  $\tilde{E}$  to more realistic potentials. We start from the observation that the surface width  $a$  of the cluster potential is an important parameter determining the supershell structure.<sup>15</sup> The basic idea is then to expand the action integrals entering the POE around the analytically known results for a potential well. It turns out that the actions can be very well approximated by linear functions in the surface parameter  $a/R_0$ , where  $R_0$  is the radius of the cluster. Thus a finite surface width leaves the frequencies in the POE unchanged and, to first order, only introduces phase shifts. Taking also the change of the Fermi energy into account, we can understand the changes in the electronic shells and supershells introduced by a soft potential surface.

The technical details of the leptodermous expansion for Woods-Saxon potentials are described in the appendix.

To simplify the notation we set  $\hbar^2/2m$  to unity, i.e. we give lengths in Bohr-radii ( $a_0$ ) and energies in Rydberg.

## II. SHELL CORRECTION METHODS

The total energy  $E(N)$  of clusters having  $N$  valence electrons can be split into a smooth and an oscillating part:

$$E(N) = \bar{E}(N) + \tilde{E}(N). \quad (1)$$

The smooth part describes the overall change in energy as the cluster size increases and is given by a liquid drop expansion<sup>23,24</sup>

$$\bar{E}(N) = a_1 N + a_2 N^{2/3} + a_3 N^{1/3} + \dots \quad (2)$$

The oscillating part is responsible for the shell structure.

The idea of shell correction methods is to give a prescription for determining  $\tilde{E}(N)$  from a one-particle calculation. These methods were pioneered by Strutinsky, who showed how the oscillating part of the total energy resulting from a Hartree-Fock calculation for atomic nuclei can be determined from the sum of the single-particle energies  $\sum \epsilon_\mu$  of a suitably defined potential.<sup>17,18</sup> A similar result holds for  $\tilde{E}(N)$  extracted from local-density functional calculations.<sup>19</sup> The latter are more common for metal clusters.<sup>9,25,26</sup> For clarity and to fix the notation we give a short outline of the relevant argument.

To find the ground state energy of a system of  $N$  electrons using density functional theory we use the Kohn-Sham formalism.<sup>27,28</sup> Starting from some electron density  $n_0(r)$  we have to solve the Kohn-Sham equations with the potential

$$V_{KS}(\vec{r}) = V_{ext}(\vec{r}) + \int d^3r' \frac{n_0(\vec{r}')}{|\vec{r} - \vec{r}'|} + V_{xc}[n_0]. \quad (3)$$

Having found the  $N$  lowest eigenstates  $\psi_\mu(\vec{r})$  with energies  $\epsilon_\mu$ , an estimate of the total energy of the system is given by the variational expression

$$E[n_0] = E_{kin}[n_0] + E_{Coul}[n_0] + E_{xc}[n_0], \quad (4)$$

where the kinetic energy is given by

$$E_{kin}[n_0] = \sum_{\mu=1}^N \epsilon_\mu - \int d^3r d^3r' \frac{n_0(\vec{r}) n(\vec{r}')}{|\vec{r} - \vec{r}'|} - \int d^3r V_{xc}[n_0] n(\vec{r}) - \int d^3r V_{ext}(\vec{r}) n(\vec{r}), \quad (5)$$

and the Coulomb energy is the sum of the Hartree energy, the interaction of the electron density with the external potential (e.g. the potential arising for the ion-cores), and the electrostatic self-energy of the ionic cores

$$E_{Coul}[n_0] = \frac{1}{2} \int d^3r d^3r' \frac{n(\vec{r}) n(\vec{r}')}{|\vec{r} - \vec{r}'|} + \int d^3r V_{ext}(\vec{r}) n(\vec{r}) + E_I. \quad (6)$$

The ‘new’ electron density  $n(\vec{r})$  in the above expressions is given by  $\sum_\mu |\psi_\mu(\vec{r})|^2$ .

Let us assume that  $n_0(\vec{r})$  was chosen close to self-consistency. Then  $n(\vec{r})$  will not differ too much from  $n_0(\vec{r})$

$$n(\vec{r}) = n_0(\vec{r}) + \delta n(\vec{r}), \quad (7)$$

and we can expand the expression for the total energy (4) in powers of  $\delta n$ . Using

$$\frac{1}{2} \int d^3r d^3r' \frac{n n}{|\vec{r} - \vec{r}'|} = -\frac{1}{2} \int d^3r d^3r' \frac{n_0 n_0}{|\vec{r} - \vec{r}'|} + \int d^3r d^3r' \frac{n_0 n}{|\vec{r} - \vec{r}'|} + \mathcal{O}^2(\delta n)$$

and

$$E_{xc}[n] = E_{xc}[n_0] + \int d^3r \underbrace{\frac{\delta E_{xc}[n_0]}{\delta n}}_{=V_{xc}[n_0](\vec{r})} \delta n(\vec{r}) + \mathcal{O}^2(\delta n)$$

we can, to first order in  $\delta n$ , write the total energy as a functional of only the initial electron density  $n_0(r)$ :

$$E = \sum_{\mu} \epsilon_{\mu} - \frac{1}{2} \int d^3r d^3r' \frac{n_0(\vec{r}) n_0(\vec{r}')}{|\vec{r} - \vec{r}'|} - \int d^3r V_{xc}[n_0](\vec{r}) n_0(\vec{r}) + E_{xc}[n_0] + E_I. \quad (8)$$

A good choice for  $n_0$  is the electron density  $n_{TF}$  resulting from an extended Thomas-Fermi (ETF) calculation. Since  $n_{ETF}(N; r)$  varies smoothly as the number of the valence electrons  $N$  in the cluster is changed, all terms in (8), except for the first one, contribute exclusively to the smooth part  $\bar{E}(N)$  of the total energy. I.e. to first order in  $\delta n$ , all electronic shell effects  $\tilde{E}(N)$  are contained in the sum of the one-particle energies  $\sum \epsilon_{\mu}$ . Hence the oscillating part  $\tilde{E}(N)$  of the total energy can be determined from the spectrum of the family  $V(N; r)$  of Kohn-Sham potentials which arise from the electron density  $n_{ETF}(r)$ . More generally, the above reasoning holds for all *families* of electron densities  $n_0(N; r)$  that are close to self-consistency and *smooth* in  $N$ .

It is common practice to immediately work with parameterized potentials  $V(N; r)$ . Usually they are chosen to fit experiments or the results of self-consistent calculations.<sup>29,5,30,10</sup> Imagining that these potentials arise from a hypothetical family of electron densities, the above arguments still apply. The prototype of such a phenomenological shell model is the Woods-Saxon potential<sup>29,5,30</sup>

$$V(N; r) = \frac{-V_0}{1 + \exp((r - r_s N^{1/3})/a)}. \quad (9)$$

Variants are the Wine-bottle potential<sup>5</sup> and the Woods-Saxon potential with asymmetric surface<sup>10</sup>

$$V(N; r) = \frac{-V_0}{1 + \exp((r - (r_s N^{1/3} + \Delta R))/f(r))}, \quad (10)$$

where  $f(r)$  is an analytical function modeling the potential near the cluster surface.

To get a feeling for the approximations involved, we compare the results of a self-consistent calculation for gallium clusters to the oscillating part of the total energy found using a family of model potentials (Fig. 1). For the self-consistent calculations we used the homogeneous, spherical jellium model.<sup>9</sup> The potentials for the one-particle calculation were obtained by fitting a function of the type (10)

$$V(N; r) = \frac{-V_0}{1 + \exp((r - R(N))/a(r))}, \quad (11)$$

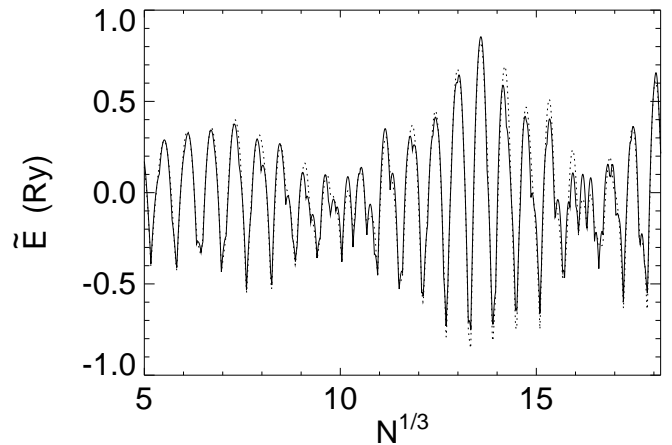


FIG. 1. Comparison of the oscillating part  $\tilde{E}(N)$  of the total energy obtained from a self-consistent calculation using the homogeneous, spherical jellium model (dotted line) to the  $\tilde{E}(N)$  extracted from the sum of the one-particle energies of a family of model potentials (full line). The model potentials are given in equation (10), with parameters  $r_s = 2.19 a_0$ ,  $V_0 = 1.04 Ry$ ,  $\Delta R = 0.73 a_0$ ,  $a_0 = 1.03 a_0$ ,  $a_1 = 1.13 a_0$ , and  $a_2 = 0.21 a_0$ .

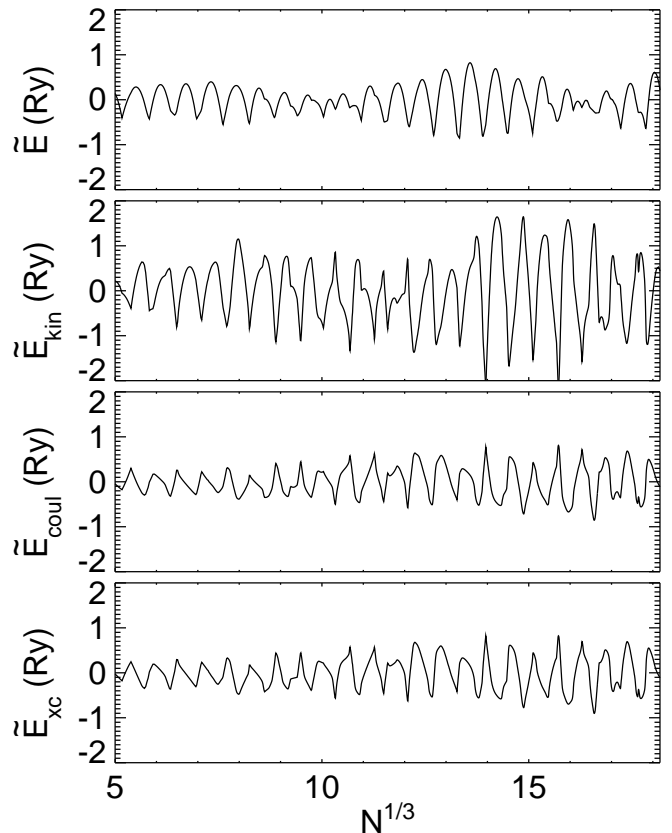


FIG. 2. Oscillating part of the total energy and of contributions to it (cf. eqn. (4)), obtained from a self-consistent calculation using the homogeneous, spherical jellium model.

where  $R(N) = r_s N^{1/3} + \Delta(r)$  and  $a(r) = a_0 + a_1 \tanh(a_2(r - R(N)))$ , to the self-consistent Kohn-Sham potentials for jellium clusters having 1500, 3000, 4500, and 6000 valence electrons.

To emphasize the importance of the smoothness of the model potentials  $V(N; r)$  in  $N$ , and to demonstrate from what subtle cancellations the electronic shell structure arises in self-consistent calculations, we show in Fig. 2 the oscillating part of the total, the kinetic, the Coulomb, and the exchange-correlation energy determined from a jellium calculation for gallium clusters. Even though in this calculation we are dealing with the self-consistent potentials and electron densities (i.e.  $\delta n = 0$ ),  $E_{kin}(N)$ , which contains the sum of the Kohn-Sham energies, is by far not the only term contributing to  $\tilde{E}(N)$ . More surprisingly the electronic shell structure as revealed by  $\tilde{E}$  cannot be found in any *single* contributions to the total energy. For the self-consistent calculation it rather is resulting from the subtle interplay of the different oscillating terms.

### III. PERIODIC ORBIT EXPANSION (POE)

As we have seen in the previous section, the oscillating part  $\tilde{E}$  of the total energy can be extracted from the sum  $\sum \varepsilon_i$  of the  $N$  lowest eigenenergies for a suitably chosen family  $V(N; r)$  of model-potentials. The determination of the electronic shell and supershell structure is thus reduced to an eigenvalue problem for these potentials. Furthermore, the radius of the clusters we are interested in is considerably larger than the de Broglie wave-length of the electrons at the Fermi level. The semiclassical approximation seems therefore well suited for solving the single-electron problem in question. In fact, for the spherical cavity, a simple rescaling of the Schrödinger equation shows that the limit  $R \rightarrow \infty$  is identical to the semiclassical limit  $\hbar \rightarrow 0$ .

The salient feature of the semiclassical approach to determining the electronic shell and supershell structure is, that it provides a natural splitting of the density of states (and consequently the total energy) into a smooth and an oscillating part. The smooth part corresponds to Thomas-Fermi theory, while the quantum corrections are given by a sum over the nontrivial periodic orbits. For an understanding of the oscillating part  $\tilde{E}$  of the total energy, we need only consider the latter.

In the present section we derive the periodic-orbit-expansion (POE) for spherical potential wells. Starting from the oscillating part  $\tilde{\rho}(k) dk$  of the density of states for a given potential  $V(r)$ , we proceed to a POE for the oscillating part  $\tilde{E}(N)$  of the total energy for a family  $V(N; r)$  of potentials. We illustrate the results by giving explicit expressions for infinite potential wells. These will be the point of reference for the leptodermous expansion discussed in Sec. V. We furthermore use the spherical cavity to assess the validity of the various approximations

made, by comparing the semiclassical results to the results obtained from numerically solving the Schrödinger equation.

#### A. POE for the density of states

We first sketch the derivation of the periodic orbit expansion of the density of states for a spherical potential well along the lines of the path-integral approach of Gutzwiller.<sup>7,31-33</sup> The starting point of the derivation is the relation between the density of states  $\rho(E)$  and the Green's function  $G(E)$

$$\rho(E) dE = -\frac{1}{\pi} \Im \text{Tr} G(E + i\epsilon) dE. \quad (12)$$

Expanding the trace in real space leads to

$$\rho(E) dE = -\frac{1}{\pi} \Im \int d^3r \lim_{\vec{r} \rightarrow \vec{r}_0} G(\vec{r}, \vec{r}_0; E + i\epsilon) dE. \quad (13)$$

Using the transformation

$$G(\vec{r}, \vec{r}_0; E) = -\frac{i}{\hbar} \int_0^\infty dt e^{iEt/\hbar} G(\vec{r}, \vec{r}_0; t) \quad (14)$$

the energy-dependent Green's function is expressed in terms of the time-dependent Green's function, which in turn can be written as a path-integral

$$G(\vec{r}, \vec{r}_0; t) = \int \mathcal{D}[\vec{r}(\tau)] e^{iS[\vec{r}(\tau)]/\hbar}. \quad (15)$$

Here the integration is over *all* paths  $\vec{r}(\tau)$  in configuration space connecting the point  $\vec{r}_0$  with  $\vec{r}$  taking a time  $t$ .  $S[\vec{r}(\tau)]$  is the classical action along such a path. In the semiclassical limit  $\hbar \rightarrow 0$  only those paths contribute for which the phase is stationary ( $\delta S = 0$ : classical paths). If the second variation of the classical action is finite ( $\delta^2 S \neq 0$ ), the path-integral becomes a Gaussian integral which can be evaluated analytically. For  $\delta^2 S = 0$  the path-integral picks up a phase factor. Thus in the semiclassical limit the path-integral (15) decomposes into a sum over classical paths<sup>34,35</sup>

$$\lim_{\hbar \rightarrow 0} G(\vec{r}, \vec{r}_0; t) = \sum_{\vec{r}_{class}(\tau)} \sqrt{\frac{\partial^2 S}{\partial \vec{r} \partial \vec{r}_0}} \exp\left(iS[\vec{r}(\tau)]/\hbar + in\pi/2\right). \quad (16)$$

The transformation (14) of the time-dependent into the energy-dependent Green's function can also be evaluated by the method of stationary phase, leading to an expression of the form

$$G(\vec{r}, \vec{r}_0; E) = \sum_{\vec{r}_{class}} \sqrt{\Delta} \exp\left(iS[\vec{r}] + \phi\right). \quad (17)$$

Again there are additional phases associated with the vanishing of the second variation.

Taking the trace (13) involves integrating over  $\vec{r}_0$  and taking the limit and  $\vec{r} \rightarrow \vec{r}_0$ . The integration over  $\vec{r}_0$  is again done in the semiclassical limit. Here the stationary-phase condition requires that the final moment equals the initial moment. The limit  $\vec{r} \rightarrow \vec{r}_0$  finally closes the orbits. Thus, since the orbits return to  $\vec{r}_0$  with the same momentum, they are closed in phase space, i.e. they are periodic. There are two distinct classes of such orbits. The first consists of only the *direct path*, the length of which vanishes as  $\vec{r} \rightarrow \vec{r}_0$ . It consequently is *local* and gives rise to the Thomas-Fermi density of states  $\bar{\rho}$ . The second class consists of periodic orbits of finite length. These *non-local* paths give rise to a quantum-correction to  $\bar{\rho}$ . Hence in the semiclassical approximation the density of states is given by the local Thomas-Fermi term with non-local corrections described by a sum over periodic orbits:

$$\rho(E) dE = \left( \bar{\rho}(E) + \tilde{\rho}(E) \right) dE. \quad (18)$$

In a spherical potential well, i.e. a potential with at most two radial turning points, all periodic orbits can be easily enumerated: A periodic orbit is characterized by the number  $\lambda$  of times it winds around the origin and the number  $\nu$  of times it traverses the outer turning point. By symmetry all orbits  $(\lambda, \nu)$  that only differ in orientation are equivalent. Fig. 3 shows some of the periodic orbits for a spherical cavity. The periodic orbits for a general spherical potential well are more rounded, but are still described by the pairs  $(\lambda, \nu)$ .<sup>5,36</sup>

The periodic orbit expansion for the oscillating part of the density of states is thus given by a sum over the families of equivalent orbits  $(\lambda, \nu)$

$$\tilde{\rho}(E) dE = \sum_{(\lambda, \nu)} A_{(\lambda, \nu)} \cos \left( \frac{S_{(\lambda, \nu)}}{\hbar} - \varphi_{(\lambda, \nu)} \right) dE, \quad (19)$$

where  $S_{(\lambda, \nu)}$  is the classical action for an orbit  $(\lambda, \nu)$  and  $\varphi_{(\lambda, \nu)}$  is the Maslov phase. The amplitude with which the orbit  $(\lambda, \nu)$  contributes is given by

$$A_{(\lambda, \nu)} = \frac{4}{\sqrt{\pi\nu}} \frac{L_{(\lambda, \nu)}}{\hbar} \frac{\partial s_r / \hbar}{\partial E} \left| \frac{\partial^2 s_r \hbar}{\partial L^2} \right|^{-1/2}, \quad (20)$$

with  $L$  denoting the angular momentum and  $s_r$  the radial action.<sup>7</sup>

For a spherical cavity of radius  $R_0$  the terms that enter the periodic orbit expansion take a simple form: The classical action of an orbit equals its length times the wavevector  $k$

$$S_{(\lambda, \nu)}(k) / \hbar = 2\nu k R_0 \sin \left( \frac{\pi\lambda}{\nu} \right), \quad (21)$$

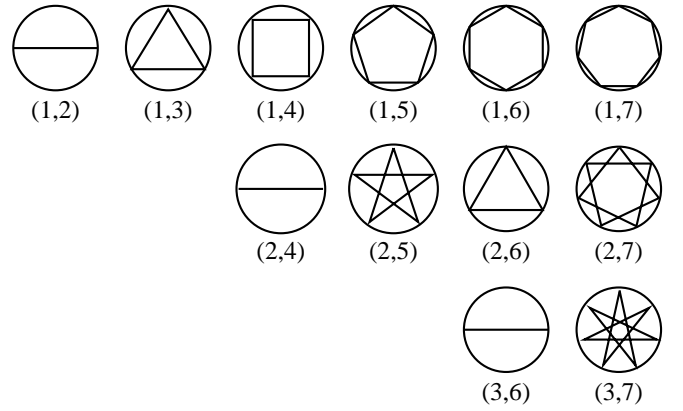


FIG. 3. Some periodic orbits for a spherical cavity. They are characterized by the pair  $(\lambda, \nu)$ , where  $\lambda$  denotes the number of times the orbit revolves around the origin before it closes on itself, and  $\nu$  is the number of vertices it has. Note that  $(n\lambda, n\nu)$  is the orbit obtained by traversing  $(\lambda, \nu)$   $n$  times.

the phase is given by

$$\varphi_{(\lambda, \nu)} = \left( \frac{3}{2}\nu + \lambda - \frac{1}{4} \right) \pi, \quad (22)$$

and the amplitude takes the form

$$A_{(\lambda, \nu)} = \sqrt{k} R_0^{5/2} \alpha_{(\lambda, \nu)} \quad (23)$$

with the dimensionless geometry-factors

$$\alpha_{(\lambda, \nu)} = \frac{2}{\sqrt{\pi\nu}} \sqrt{\sin \left( \frac{\pi\lambda}{\nu} \right) \sin \left( \frac{2\pi\lambda}{\nu} \right)}. \quad (24)$$

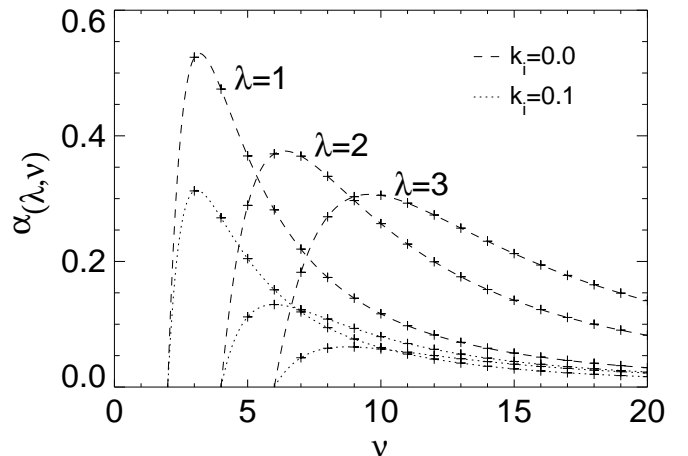


FIG. 4. Amplitudes  $\alpha_{(\lambda, \nu)}$  with which the periodic orbits  $(\lambda, \nu)$  contribute to the oscillating part  $\tilde{\rho}$  of the density of states. Shown are the amplitudes (crosses) for no ( $k_i = 0$ ) and for an intermediate ( $k_i = 0.1$ ) smoothing. To guide the eye, the amplitudes for a given number of turns are connected by lines.

The  $\alpha_{(\lambda,\nu)}$  determine the relative importance of the periodic orbits in the POE (19). Their values for the first few periodic orbits are shown in Fig. 4 ( $k_i = 0$ ). We note that the amplitudes for the linear orbits ( $\lambda, 2\lambda$ ) vanish. This can be understood by a simple dimensional argument.<sup>6</sup> Since the sum in the POE is over *all* periodic orbits, the number of different but equivalent orbits ( $\lambda, \nu$ ) will be reflected in the amplitude  $\alpha_{(\lambda,\nu)}$ . To parameterize all the different orientations of the linear orbits it is sufficient to give the coordinates of one of their outer turning points. Since for a spherical potential well the outer turning point lies on the surface of a sphere, the manifold of the linear orbits has dimension 2. All the higher orbits are not linear but lie in a plane, so we need an additional parameter to fix the orientation of this plane. The manifold of the planar orbits are therefore 3-dimensional ('there are many more planar than linear orbits'). Thus the linear orbits do not contribute to the leading order of the periodic orbit expansion. The largest amplitudes are found for the triangular (1, 3) and the square (1, 4) orbit. The contribution from other orbits is, however, still large, i.e. one has to include many periodic orbits in a partial summation of (19) before one obtains a result close to  $\tilde{\rho}$ . This slow convergence is to be expected since the density of states for a finite system is given by a sum of  $\delta$ -functions which cannot easily be reproduced by a sum of analytical functions. To improve the convergence of the expansion one can replace the  $\delta$ -peaks in the DOS by Lorentzians of width  $\gamma$ . This corresponds to introducing a complex wavevector  $k = k_r + ik_i$  in the periodic orbit expansion. As can be seen from Fig. 4, a finite value of  $k_i$  serves to reduce the contribution of higher orbits considerably. However, since the shell and supershell structure in metal clusters is not directly linked to  $\tilde{\rho}$  but rather to the variations  $\tilde{E}$  in the total energy, we proceed to derive a periodic orbit expansion for  $\tilde{E}$ . As we will see, such an expansion converges much more rapidly than that for the density of states. We therefore need not introduce any smoothing.

### B. POE for the total energy

To find a periodic orbit expansion for the oscillating part  $\tilde{E}$  of the total energy using the POE for  $\tilde{\rho}$ , we start from the integral

$$E(N) = \int_0^{E_F(N)} E \rho(N; E) dE, \quad (25)$$

where the Fermi energy  $E_F(N)$  is fixed by the number of electrons  $N$  in the cluster

$$N = \int_0^{E_F(N)} \rho(N; E) dE. \quad (26)$$

Similar equations hold in Thomas-Fermi theory. Subtracting the corresponding Thomas-Fermi expression from (26) we find

$$0 = \int_{\tilde{E}_F(N)}^{E_F(N)} \tilde{\rho}(N; E) dE + \int_0^{E_F(N)} \tilde{\rho}(N; E) dE. \quad (27)$$

Since the smooth part of the density of states does not vary much over the small interval  $\tilde{E}_F \dots E_F$ , we can approximate the first integral in the above expression by  $\tilde{E}_F(N) \tilde{\rho}(N; E_F)$ . We then can use the above equation to solve for  $\tilde{E}_F(N)$ . In a similar fashion we can approximate the difference of (25) and its Thomas-Fermi counterpart by

$$\tilde{E}(N) \approx \tilde{E}_F(N) E_F(N) \tilde{\rho}(N; E_F) + \int_0^{E_F(N)} E \tilde{\rho}(N; E) dE.$$

Using the approximate expression for  $\tilde{E}_F$  from eqn. (27) we find

$$\tilde{E}(N) \approx \int_0^{E_F(N)} (E - E_F(N)) \tilde{\rho}(N; E) dE. \quad (28)$$

Since the integrand vanishes at the upper limit of integration it is now possible to approximate  $E_F(N)$  by its Thomas-Fermi counterpart  $\tilde{E}_F(N)$ . Integrating by parts we finally arrive at

$$\tilde{E}(N) \approx - \int_0^{\tilde{E}_F(N)} dE \int_0^E dE' \tilde{\rho}(N; E'). \quad (29)$$

i.e. to find an approximation to the oscillating part of the total energy we have to integrate twice over the oscillating part of the density of states.

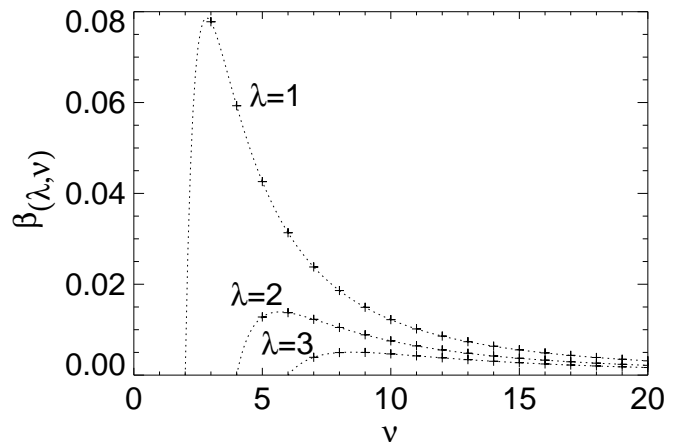


FIG. 5. Amplitudes  $\beta_{(\lambda,\nu)}$  with which the periodic orbits ( $\lambda, \nu$ ) contribute to the oscillating part  $\tilde{E}$  of the total energy. Comparison with Fig. 4 shows that the dominance of the short, planar orbits, which for the oscillating part  $\tilde{\rho}$  of the density of states has to be enforced by introducing an artificial smoothing  $k_i$ , occurs naturally for  $\tilde{E}$

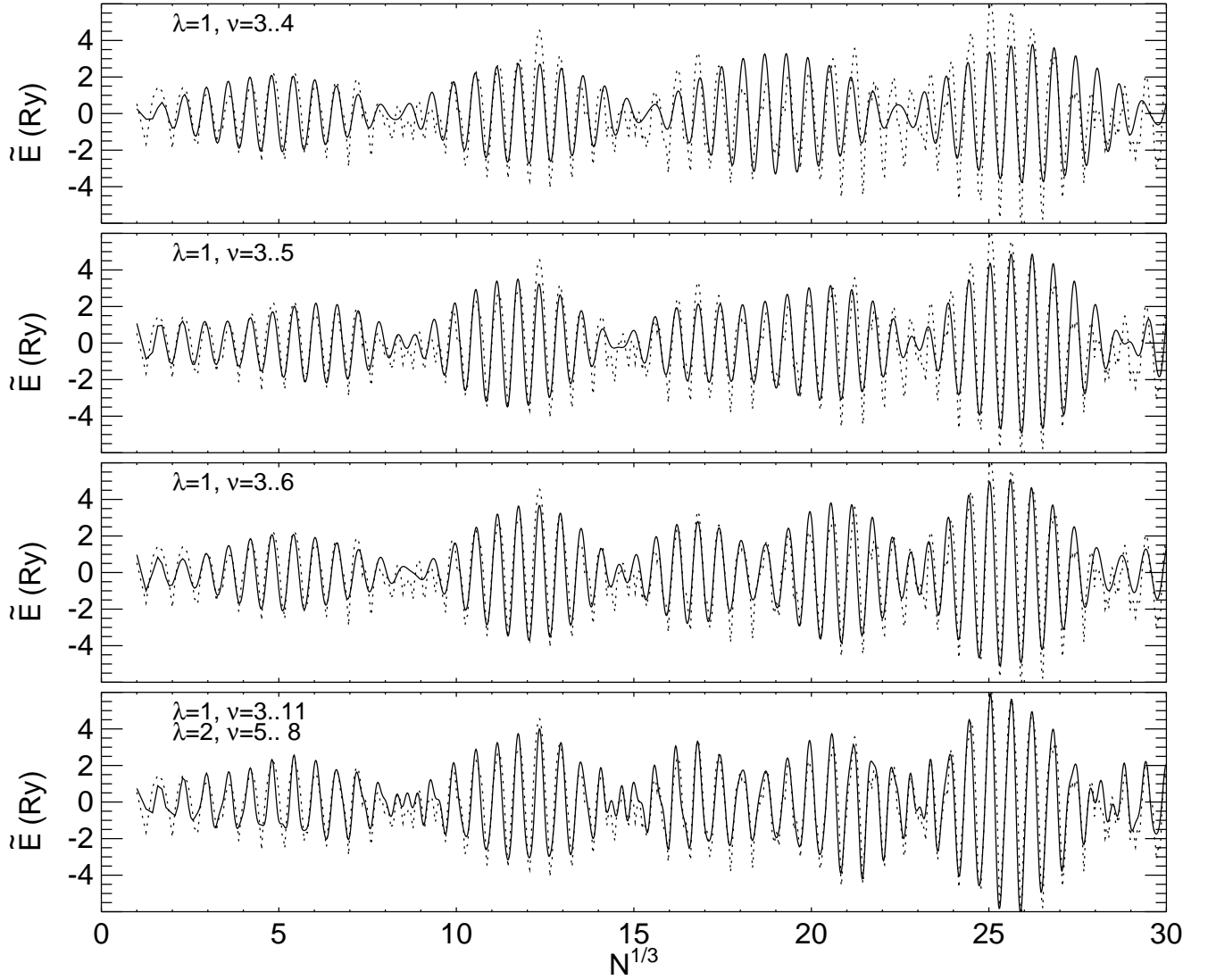


FIG. 6. Comparison of the periodic orbit expansion for the oscillating part  $\tilde{E}$  of the total energy to the quantum mechanical result for spherical cavities. The plots show  $\tilde{E}$  obtained from a truncated periodic orbit expansion, including more and more orbits. The orbits were included in the order of decreasing amplitude: (1, 3), (1, 4), (1, 5), (1, 6), (1, 7), (1, 8), (1, 9), (2, 6), (2, 5), (2, 7), (1, 10), (2, 8), (1, 11). The  $\tilde{E}_{QM}$  from the quantum mechanical calculation is shown by the dotted line.

Using (29) and (19) we find for spherical cavities of radius  $R_0(N)$  the expansion

$$\tilde{E}(N) \approx \sqrt{\bar{k}_F R_0} \bar{k}_F^2 \sum_{(\lambda, \nu)} \frac{4\alpha_{(\lambda, \nu)}}{\hat{S}_{(\lambda, \nu)}^2} \cos\left(\hat{S}_{(\lambda, \nu)} \bar{k}_F R_0 - \varphi_{(\lambda, \nu)}\right) \quad (30)$$

which is similar to (19), the main difference being the change in the amplitudes: Due to the twofold integration the amplitudes are divided by the square of the dimensionless classical action  $\hat{S}_{(\lambda, \nu)} = S_{(\lambda, \nu)} / (\hbar k R_0)$ . The new geometry factors are thus given by

$$\beta_{(\lambda, \nu)} := \frac{4\alpha_{(\lambda, \nu)}}{\hat{S}_{(\lambda, \nu)}^2}. \quad (31)$$

They are plotted in Fig. 5. A comparison with the  $\alpha_{(\lambda, \nu)}$

(Fig. 4) shows how the contributions of the long orbits (with large classical action, see eqn. (21)) to the POE for  $\tilde{E}(N)$  are reduced. This improvement of convergence can be understood intuitively since  $E(N)$  is continuous, while the density of states is highly singular, being a forest of  $\delta$ -functions.

To check the approximations made in the derivation of eqn. (29) we compare the results of a truncated periodic orbit expansion for  $\tilde{E}$  with the oscillating part  $\tilde{E}_{QM}$  of the total energy derived from a quantum mechanical calculation. Such a comparison for spherical cavities of radius  $R_0 = N^{1/3}$  is shown in Fig. 6. It turns out that the truncated POEs reproduce  $\tilde{E}_{QM}$  very well, even if only a few periodic orbits are included. In particular the first two supershells can be described using only the triangular and square orbit. However, for even larger sizes

$N$  it seems that higher orbits are needed to describe the structure in  $\tilde{E}_{QM}$ . We note that due to its nature of being a semiclassical result, the periodic orbit expansion for  $\tilde{E}$  will not converge to  $\tilde{E}_{QM}$  but to its semiclassical approximation.

#### IV. LATTICE CONTRACTION

As a first application of the periodic orbit expansion for the oscillating part of the total energy we look at the effects of a lattice contraction on the electronic shells and supershells. Extended X-ray absorption fine structure (EXAFS) measurements on small clusters adsorbed on some substrate indicate that the next-neighbor distance might decrease with decreasing cluster size.<sup>21,22</sup> Such a contraction of the cluster is also suggested by a continuum description of large clusters: Since for small clusters the surface-to-volume-ratio increases, the surface tension, which has the tendency to compress the cluster, will become more and more important. Neglecting this finite-size effect, a spherical cluster of  $N$  atoms will have a radius  $R_0 = r_s N^{1/3}$ , where  $r_s$  is the Wigner-Seitz radius of the bulk material. Acting against the compressibility  $\kappa$ , the surface tension  $\sigma$  will reduce the cluster radius:

$$\frac{\Delta R}{R_0} = -\frac{2\kappa\sigma}{3} \frac{1}{R_0}. \quad (32)$$

Thus we expect the radius of a cluster of  $N$  atoms to be given by

$$R(N) = R_0 + \Delta R = r_s N^{1/3} + \Delta R \quad (33)$$

with a size-independent contraction  $\Delta R$ . A rough estimate using the compressibilities and surface tensions of the liquid alkali metals just above the melting point gives  $\Delta R/r_s \approx 0.1$ .

To see how the electronic shells and supershells are affected by such a lattice contraction we first turn to the special case of the spherical cavity. Inspecting eqn. (30) we see that the periods of the oscillations in  $\tilde{E}$  are determined by the product  $\bar{k}_F R$ , while all other quantities in the argument of the cosine are independent of cluster size.  $\bar{k}_F R$  should, however, depend only weakly on the cluster radius, since we expect a decrease in cluster radius to be compensated by an increase in the Fermi energy. For the spherical cavity we actually have

$$\bar{k}_F R = b_1 N^{1/3} + b_2 + \mathcal{O}(N^{-1/3}) \quad (34)$$

with  $b_1 = (9\pi/4)^{1/3}$  and  $b_2 = 3\pi/8$ . I.e. for spherical cavities  $\bar{k}_F(N)R(N)$  is independent of  $R(N)$  and therefore the *position* of the electronic shells and supershells are *independent* of the actual cluster radius  $R(N)$ .

Looking again at eqn. (30) we notice that in the overall prefactor of the periodic orbit expansion we have

an isolated factor  $k_F^2$ . Since the Fermi energy obviously depends on the cluster size, we expect the *amplitude* of  $\tilde{E}$  to be affected by a lattice contraction. For  $R(N) = r_s N^{1/3} + \Delta R$  we find from (34)

$$\bar{k}_F(N)r_s = b_1 + \left( b_2 - b_1 \frac{\Delta R}{r_s} \right) + \mathcal{O}(N^{-2/3}). \quad (35)$$

Thus for small cluster sizes the amplitude of the shell oscillations will increase with increasing lattice contraction.

To check in how far the above findings also hold for more realistic cluster potentials, we have calculated the oscillating part of the total energy from the eigenvalues of a family of Woods-Saxon potentials. The parameters were chosen to resemble the potentials from jellium calculations for sodium. In Fig. 7 we compare  $\tilde{E}_{QM}$  for contracted/expanded clusters with clusters of radius  $R(N) = r_s N^{1/3}$ . We find that even for unphysically large contractions/expansions ( $\Delta R/r_s = \pm 0.5$ ) the location of the electronic shells and supershells is hardly changed, while for small numbers of atoms  $N$  the amplitude of  $\tilde{E}(N)$  increases/decreases for the contracted/expanded clusters.

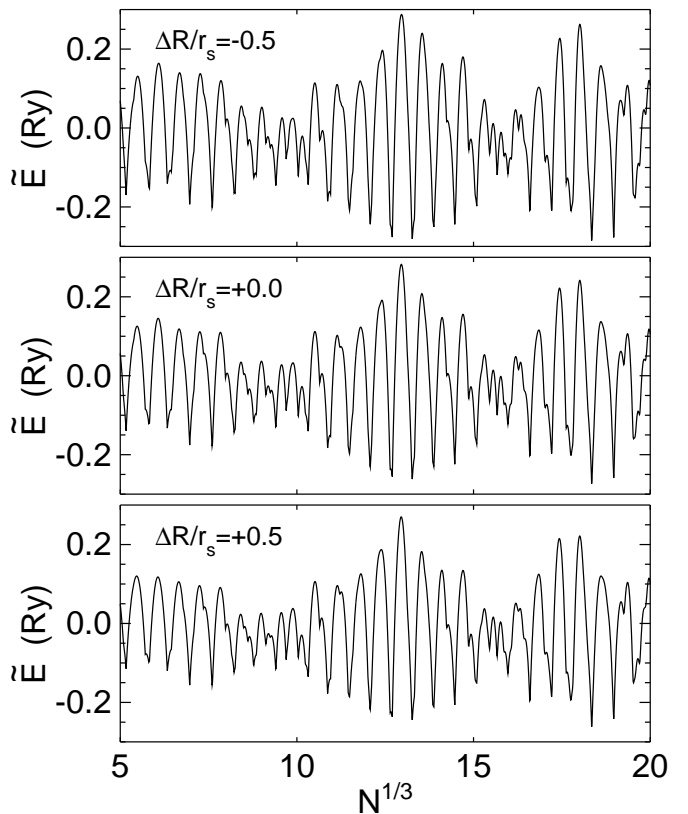


FIG. 7. Oscillating part  $\tilde{E}$  of the total energy for Woods-Saxon potentials  $V(r) = -V_0/(1 + \exp((r - R(N))/a))$  with lattice contraction  $R(N) = r_s N^{1/3} + \Delta R$ . The parameters  $r_s = 3.93 a_0$ ,  $V_0 = 0.46 Ry$ , and  $a = 0.94 a_0$  were chosen to resemble the potential for sodium-jellium clusters.

## V. LEPTODERMOUS EXPANSION

So far we only have explicit expressions of the periodic orbit expansion for cavity potentials. We now want to extend the POE to more realistic potentials  $V(r)$ , like the Woods-Saxon potential (eqn. (9)). These potentials differ from the cavity potential by having a surface of finite width  $a$ . Since the slope of the cavity potential is infinite at the surface,  $\delta V(r) = V(r) - V_{cavity}$  is never a small quantity. But, rewriting integrals over  $V(r)$  in a suitable way, we can use the surface width  $a$  as an expansion parameter.

From (30) we see that we need to find expressions for (i) the action integral  $\hat{S}_{(\lambda,\nu)}$  for orbits  $(\lambda,\nu)$ , (ii) the Fermi wave-vector  $\bar{k}_F$  in Thomas-Fermi approximation, and (iii) the phases  $\varphi_{(\lambda,\nu)}$ . For this we proceed as follows. We first introduce the idea of the leptodermous expansion for integrals over the potential  $V(r)$  for classical action. We find an expansion

$$\hat{S}_{(\lambda,\nu)} = \hat{S}_{(\lambda,\nu)}^{cavity} + 2\nu \hat{I}_s \frac{a}{R_0}. \quad (36)$$

Then we estimate the change in  $\bar{k}_F r_s$  due to the finite surface width. To first order in  $a$  we find

$$\bar{k}_F r_s = \left(\frac{9\pi}{4}\right)^{1/3} + \left(c_1 + c_2 \frac{a}{r_s}\right) N^{-1/3}. \quad (37)$$

Finally we estimate the phase  $\varphi_{(\lambda,\nu)}$ . Rearranging terms in powers of  $N^{1/3}$ , the argument of the cosine in eqn. (30) then reads

$$\begin{aligned} & \left(\frac{9\pi}{4}\right)^{1/3} \hat{S}_{(\lambda,\nu)}^{cavity} N^{1/3} \\ & + \hat{S}_{(\lambda,\nu)}^{cavity} \left(c_1 + c_2 \frac{a}{r_s}\right) + 2\nu \left(\frac{9\pi}{4}\right)^{1/3} \hat{I}_s \frac{a}{r_s} - \varphi_{(\lambda,\nu)}, \end{aligned} \quad (38)$$

i.e. the first order terms in the leptodermous expansion give rise to a *phase shift* in the periodic orbit expansion, while the frequencies  $S_{(\lambda,\nu)}^{cavity}$  are unchanged.

### A. Classical action

To introduce the basic idea of the leptodermous expansion we first consider potentials that differ from the cavity potential only in a small region around the cluster surface, say for  $r > R_0 - \alpha$ . It is then straightforward to split the radial integrals into two parts, one integral over the interior  $r = 0 \dots R_0 - \alpha$  and one over the surface region  $r = R_0 - \alpha \dots r_{out}$ . Thus the radial action can be rewritten as

$$\begin{aligned} s_r/\hbar &= \int_{r_{in}}^{r_{out}} \sqrt{E - V(r) - L^2/r^2} dr \\ &= \int_{r_{in}}^{R_0 - \alpha} \sqrt{\cdot} dr + \int_{R_0 - \alpha}^{r_{out}} \sqrt{\cdot} dr. \end{aligned} \quad (39)$$

The first integral is the action integral for a spherical cavity of radius  $R_0 - \alpha$ , which we know already. The second integral can, in general, not be solved analytically. But for small  $\alpha$  we can get a good approximation by neglecting the variation of the angular momentum term over the small interval  $[R_0 - \alpha, r_{out}]$ , e.g. setting  $L^2/r^2$  to  $L^2/R_0^2$ .

Realistic cluster potentials are not that simple. In a Woods-Saxon potential there is no obvious point, that separates bulk from surface. We can still make the same ansatz by choosing some small  $\alpha$ , but we have to make sure that our result does not depend on our specific choice. To do so, we add and subtract the integral  $\int_0^{R_0 - \alpha} \sqrt{E + V_0 - L^2/R_0^2} dr$  to (39). Using  $V(r) \approx -V_0$  for  $r < R_0 - a$  we find

$$\begin{aligned} s_r/\hbar &\approx \int_{r_{in}}^{R_0 - \alpha} \sqrt{E + V_0 - L^2/r^2} dr \\ &+ \int_0^{r_{out}} \sqrt{E - V(r) - L^2/R_0^2} dr \\ &- \int_0^{R_0 - \alpha} \sqrt{E + V_0 - L^2/R_0^2} dr \end{aligned} \quad (40)$$

Using again  $L^2/r^2 \approx L^2/R_0^2$  for  $r \in [R_0 - \alpha, r_{out}]$ , we can extend the upper limit of integration of the first and third integral from  $R_0 - \alpha$  to  $r_{out}$ . The first integral is then the radial action for the cavity potential, the two other terms give the correction due to the soft surface of the potential  $V(r)$ . Introducing dimensionless quantities  $\hat{a} = a/R_0$ ,  $\hat{s} = s/kR_0$ , and  $\hat{L} = L/\hbar k R_0$ , with  $k = \sqrt{E + V_0}$ , and expanding in powers of the reduced surface-width  $\hat{a}$ , we get

$$\hat{s}_r(P, \hat{L}, \hat{a}) = \hat{s}_r^{cavity}(\hat{L}) + \hat{I}_s(P, \hat{L}) \hat{a} + \mathcal{O}(\hat{a}^2), \quad (41)$$

where  $P = \sqrt{(E + V_0)/V_0}$ , and  $\hat{s}_r^{cavity}(\hat{L}) = \sqrt{1 - \hat{L}^2} - \hat{L} \arccos(\hat{L})$  is the reduced radial action for a spherical cavity. In appendix A it is shown how to calculate  $\hat{I}_s$  for a Woods-Saxon potential.

Given the expansion for the radial action, we now proceed to calculate the action for a periodic orbit  $(\lambda, \nu)$

$$\hat{S}_{(\lambda,\nu)} = 2\nu \hat{s}_r + 2\pi\lambda \hat{L}_{(\lambda,\nu)}. \quad (42)$$

The angular momentum  $L_{(\lambda,\nu)}$  associated with the orbit can be determined from the periodicity condition: In order to close after  $\lambda$  turns and having traversed the outer turning point  $\nu$  times, the angle  $\Phi$  swept during one radial oscillation must be  $\pi\lambda/\nu$ . With (41) this leads to

$$\frac{\pi\lambda}{\nu} = \Phi = -\frac{\partial \hat{s}_r}{\partial \hat{L}} = \arccos(\hat{L}) - \frac{\partial \hat{I}_s}{\partial \hat{L}} \hat{a} + \mathcal{O}(\hat{a}^2). \quad (43)$$

Taking the derivative with respect to  $\hat{a}$  at  $\hat{a} = 0$ , we can solve for the first order correction in the reduced angular momentum:

$$\hat{L}_{(\lambda,\nu)} = \hat{L}_{(\lambda,\nu)}^{cavity} - \sqrt{1 - (\hat{L}_{(\lambda,\nu)}^{cavity})^2} \frac{\partial \hat{I}_s(P, \hat{L}_{(\lambda,\nu)}^{cavity})}{\partial \hat{L}} \hat{a}. \quad (44)$$

We can use this to expand  $\hat{s}_r^{cavity}(\hat{L})$  in (41) around  $\hat{L}_{(\lambda,\nu)}^{cavity} = \cos(\pi\lambda/\nu)$ . Inserting into (42) we see that the first order correction in  $\hat{s}_r^{cavity}$  cancels that coming from  $\hat{L}$ . Thus to first order in  $\hat{a}$  the reduced action for a periodic orbit  $(\lambda, \nu)$  is given by

$$\hat{S}(P, \hat{L}_{(\lambda,\nu)}, \hat{a}) = \hat{S}_{(\lambda,\nu)}^{cavity} + 2\nu \hat{I}_s(P, \hat{L}_{(\lambda,\nu)}^{cavity}) \hat{a} + \mathcal{O}(\hat{a}^2). \quad (45)$$

This result is independent of the specific form of the potential, as long as an expansion (41) of the radial action exists.

### B. Fermi level

We now turn to the problem of determining the Fermi wavevector  $\bar{k}_F$  in the extended Thomas-Fermi approximation for a cluster with  $N$  electrons. In an infinite system we have  $\bar{k}_F r_s = (9\pi/4)^{1/3}$ . For a finite system there will be corrections arising from the surface

$$\bar{k}_F r_s = (9\pi/4)^{1/3} + c_F N^{-1/3} + \dots \quad (46)$$

The surface term can be calculated from the quantum mechanical scattering phase  $\varphi(k)$  at the surface potential<sup>37,38</sup>

$$c_F = -\frac{3}{\bar{k}_F^2} \int_0^{\bar{k}_F} \left( \frac{\pi}{4} - \varphi(k) \right) k dk. \quad (47)$$

Assuming that the potential is slowly varying at the outer turning point, we can determine the scattering phase from the classical action.

For a slowly varying potential the WKB wave function in the region  $r \ll R_0 - a$  where the potential is practically constant is<sup>33</sup>

$$u_{WKB}(r) \propto \cos \left( \int_r^{r_{out}} k(r) dr - \frac{\pi}{4} \right), \quad (48)$$

while the quantum mechanical wave function is

$$u_{QM}(r) \propto \cos(k(R_0 - r) - \varphi(k)). \quad (49)$$

In the semiclassical limit, i.e. for large  $R_0$ , both expressions should be equal. Choosing  $r = 0$ , we find

$$\varphi(k) = - \left( \int_0^{r_{out}} k(r) dr - k R_0 \right) + \frac{\pi}{4} \quad (50)$$

$$= \frac{\pi}{4} - \hat{I}_s(P, 0) k a + \mathcal{O}(a^2), \quad (51)$$

where in the last equation we have used the linearization (41) of the radial action. We note that for  $L = 0$  the

leptodermous expansion is exact, i.e. there are no higher order terms in (41). From (47) the surface parameter thus is

$$c_F = -\frac{3a}{\bar{k}_F^2} \int_0^{\bar{k}_F} \hat{I}_s(P(k), 0) k^2 dk \quad (52)$$

$$= - \left( \frac{9\pi}{4} \right)^{1/3} \hat{I}_N(P_F) \frac{a}{r_s}. \quad (53)$$

The analytic expression of  $\hat{I}_N$  for Woods-Saxon potentials is calculated in appendix A (eqn. (A10)).

It is interesting to note that we can obtain the same result from expanding the Thomas-Fermi integral in powers of  $a$

$$\begin{aligned} N &= \int_0^{r_{out}} (\bar{E}_F - V(R))^{3/2} r^2 dr \\ &= \frac{(\bar{k}_F R_0)^3}{3} + (\bar{k}_F R_0)^3 \hat{I}_N \hat{a} \end{aligned} \quad (54)$$

and solving for  $\bar{k}_F r_s$ . In fact, in the approximation considered here, both approaches are equivalent.

It is important to realize that the above reasoning involves two, possibly conflicting approximations. In the ansatz (48) for the semiclassical wave function we have assumed that the potential is slowly varying, i.e. that  $a$  is large enough, while for the leptodermous expansion of the radial action of the orbits with  $L \neq 0$  we require that  $a$  is small.

To see how well the expression (52) for  $c_F$  works, we compare it to the surface term obtained by fitting the Fermi wavevector  $k_F(N)$  calculated quantum mechanically for Woods-Saxon potentials holding 50...8000 electrons. As expected our approximation approaches the quantum mechanical result in the limit of large surface width  $a$  (slowly-varying-potential regime). But it also works quite well for relatively small  $a$ . For very small  $a$  the approximation of course breaks down, since our ansatz does not describe the crossover from the slowly-varying-potential regime to the potential step at  $a = 0$ , for which the phase in  $u_{WKB}(r)$  is  $\arctan(\kappa/k)$  instead of  $\pi/4$ . Using this phase in the above derivation, we recover the correct surface parameter for the finite potential well.

Since for larger  $a$  the approximation to  $c_F$  runs roughly parallel to the true value of the surface term, one might improve the accuracy of the leptodermous expansion by shifting (52) by a constant ( $a$ -independent) amount  $c_1$ . Since the Woods-Saxon potential in one dimension is exactly solvable<sup>39,40</sup>, this is straightforward.

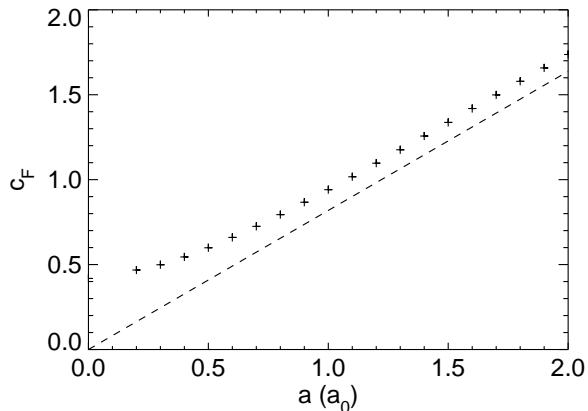


FIG. 8. Surface term  $c_F$  in the asymptotic expansion of  $\bar{k}_F r_s$  (cf. eqn. (46)) as a function of the surface width  $a$  for a Woods-Saxon potential. The potential parameters are  $V_0 = 0.45 Ry$ ,  $r_s = 4 a_0$ . The crosses were obtained by fitting the Fermi wavevector from full quantum mechanical calculations for clusters with 50...8000 electrons. The dashed line gives the estimate of  $c_F$  as given by eqn. (52).

### C. Maslov phase

For separable potentials the Maslov phase is determined by the phases that the semiclassical wave function picks up at the classical turning points. For a given periodic orbit  $(\lambda, \nu)$  there are  $2\lambda$  turning points in the  $\vartheta$ -motion, each contributing a phase  $\pi/2$ . The same orbit also has  $2\nu$  radial turning points. The  $\nu$  inner turning points see the smooth centrifugal potential, hence also contribute  $\pi/2$ . The phase  $\phi_{out}$  at the outer turning point depends on the shape of the potential  $V(r)$  at the surface. The Maslov phase for the orbit is then given by

$$\varphi_{(\lambda, \nu)} = [(1/2 + \phi_{out}/\pi)\nu + \lambda - 1/4]\pi. \quad (55)$$

For a step potential, we can find  $\phi_{out}$  by matching the semiclassical radial wave function to the boundary condition at the turning point. For an infinite potential well  $\phi_{out} = \pi$ , while for a well of depth  $V_0$   $\phi_{out} = 2 \arctan(\kappa/k)$ , where  $\kappa = \sqrt{V_0 - k^2}$ .

For a slowly varying potential, on the other hand, the standard result obtained by linearizing the potential around the classical turning point is  $\phi_{out} = \pi/2$ .

The Woods-Saxon potential for a typical cluster has a surface width of  $a = 0.5 \dots 1.5 a_0$ . As we have seen above, for such values of  $a$  the potential is already in the slowly-varying-regime. We therefore use

$$\varphi_{(\lambda, \nu)} = [\nu + \lambda - 1/4]\pi. \quad (56)$$

### D. Leptodermous POE

We can now collect all the contributions to calculate the effect of a softening of the potential at the surface on

the periodic orbit expansion (30) of the oscillating part  $\tilde{E}$  of the total energy. The frequencies associated with the periodic orbits turn out to be unchanged, to first order there is only a phase shift:

$$\tilde{E}(N) \propto \sum_{(\lambda, \nu)} \beta_{(\lambda, \nu)} \cos \left( \left( \frac{9\pi}{4} \right)^{1/3} \hat{S}_{(\lambda, \nu)}^{cavity} N^{1/3} + \Delta\Phi_{(\lambda, \nu)} \right) \quad (57)$$

with

$$\Delta\Phi_{(\lambda, \nu)} = \left( \frac{9\pi}{4} \right)^{1/3} \left[ 2\nu \hat{I}_s(P, \hat{L}) - \hat{S}_{(\lambda, \nu)}^{cavity} \hat{I}_N(P) \right] \frac{a}{r_s} - [\nu + \lambda - 1/4]\pi. \quad (58)$$

We stress again that we have made two, possibly conflicting approximations. On the one hand, the leptodermous expansion of the radial action relies on the fact that the surface width  $a$  is small, while a slowly-varying-potential assumption enters in the calculation of the scattering phase. To see how the above expression works in practical calculations, we compare the periodic orbit expansion (57) with the result of quantum mechanical calculations for Woods-Saxon potentials with parameters typical for alkali metal cluster, see Fig. 9. The agreement is surprisingly good. The shift of the supernodes with increasing surface width is well described, and also the shell oscillations are quite well reproduced. We could get even better agreement by numerically fitting the action integrals (see Fig. 11) and the surface coefficient  $c_F$  with *linear* functions in  $a$ . In that sense the concept of the surface introducing just a phase-shift in the periodic orbit expansion seems to be applicable even beyond the range where the analytical expressions from the leptodermous expansion are good approximations.

Taking only triangular and square orbits into account, the shift in the shell (supershell) oscillations is given by  $(\Delta\Phi_{(1,3)} \pm \Delta\Phi_{(1,4)})/2$ . As we can see from (58), the contributions coming from  $c_F$  almost cancel for the supershells, since the classical actions for the triangular and the square orbit are so similar. Because of this cancellation of errors the shift of the supershells with the surface width is very well described in the leptodermous expansion.<sup>16</sup> The shell oscillations are more sensitive to approximations. But the most important feature, namely that shells are hardly affected by changes in the surface width, is also well reproduced.

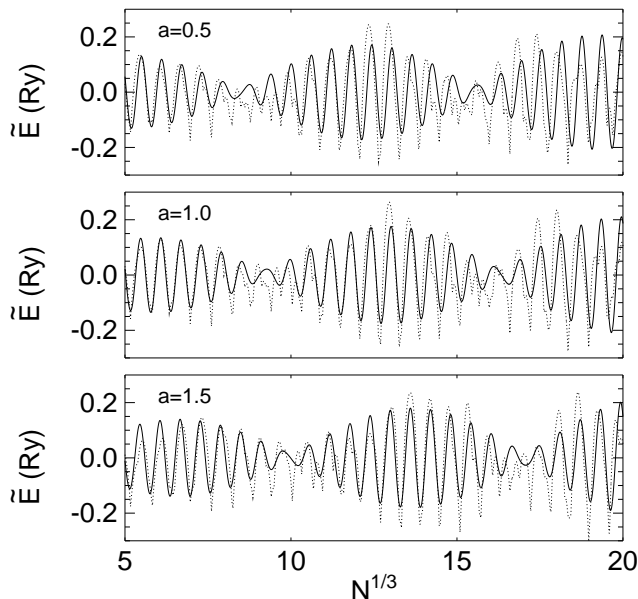


FIG. 9. Oscillating part  $\tilde{E}$  of the total energy for Woods-Saxon potentials  $V(r) = -V_0/(1 + \exp((r - R(N))/a))$  with different surface width  $a$ .  $R(N) = N^{1/3}r_s$  with  $r_s = 4a_0$  and  $V_0 = 0.45$ . The dotted lines give the results of quantum mechanical calculations. The full lines are obtained from the leptodermous expansion (57), including only triangular and square orbits.

## VI. CONCLUSIONS

Using periodic orbit theory we see that the electronic supershell structure is a sensitive probe for the surface of clusters. It turns out that possible lattice contractions, which at first sight seem like important surface effects, hardly influence the electronic shell structure. There is a pronounced effect of the width of the surface region on the position of the supershells. The leptodermous expansion around the limiting case of a spherical cavity provides a natural framework for understanding the shift of the supershells with increasing surface width. A particularly nice feature of the leptodermous expansion, as we have presented it here, is the fact that the expansion of the radial action is the *only* input we need. All other quantities entering the periodic orbit expansion can be easily derived from the radial action. It is therefore straightforward to apply the formalism to other types of potentials.

The shift in the electronic supershells that is described by the leptodermous expansion has been seen in numerical studies of  $\tilde{E}$  for soft potentials<sup>30</sup> and it has been used to understand the results of self-consistent jellium calculations.<sup>16</sup> The observations of a shift proportional to the surface width can be regarded as a signature of the leptodermous regime. Eventually the leptodermous approximation will break down, since for extremely soft potentials the planar orbits with  $\lambda = 1$  cease to exist.

For such potentials star orbits become the leading terms, which causes a change in the *frequency* of the shell and supershell oscillations<sup>41,42</sup> as opposed to a change in the *phase* only.

It is interesting to compare the leptodermous expansion of the semiclassical sum over periodic orbits with the quantum mechanical perturbation theory. In quantum mechanics we would expect perturbation theory to break down when the shifts of the energy levels are of the order of their spacing. For the potentials we have considered here the change in the energy levels is quite large, especially for the levels with high angular momentum, which are most sensitive to the potential at the surface. Typical shifts of the energy levels with the surface width  $a$  for a set of Woods-Saxon potentials are shown in Fig. 10. Nevertheless, the electronic shells are not that strongly affected, because the levels with large angular momentum, which are mostly responsible for the oscillations in the total energy, are shifted by large, but similar amounts. It seems that since the semiclassical periodic orbit expansion does not deal with individual energy levels but only with the collective changes in the spectrum, it works so well, even for large surface widths  $a$ .

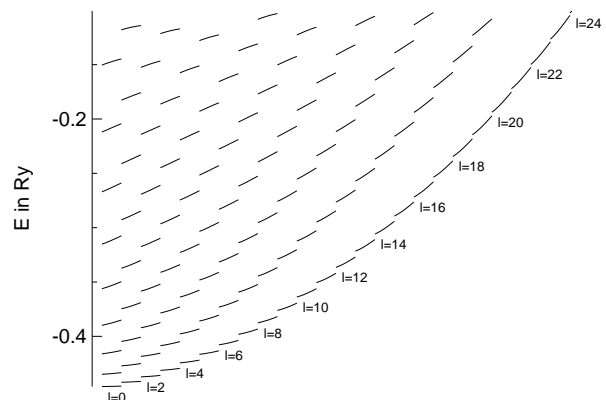


FIG. 10. Shift in the energy levels  $\varepsilon_{n,l}$  for Woods-Saxon potentials with different surface-width  $a$ . The parameters for the potentials are  $V_0 = 0.45 Ry$ ,  $R_0 = 50a_0$  and  $a = 0.5 \dots 1.5a_0$ . For given angular momentum  $l$  the levels are plotted one above the other. Each line shows  $\varepsilon_{n,l}$  as a function of  $a$ , with  $a$  increasing from left to right.

The leptodermous expansion should also be of use in understanding experiments probing the transport properties of high-mobility semiconductor microstructures.<sup>43</sup> The oscillations in the conductance of quantum dots are quite well described by simple cavity potentials. At first sight this seems surprising since the confining potential of a quantum dot is expected to be rather smooth. However, if these potentials are still in the leptodermous regime, it is clear that calculations using simple cavity potentials (or billiards) already describe the qualitatively correct physics.

## ACKNOWLEDGMENTS

It is a pleasure to thank O. Gunnarsson for his invaluable advice. Helpful discussions with T. P. Martin and M. Brack are gratefully acknowledged. A. Burkhardt, A. Schuhmacher, and K. Rößmann did a great job supporting us with Computer Algebra Tools.

## APPENDIX A: LEPTODERMOUS EXPANSION FOR A WOODS-SAXON POTENTIAL

In this appendix we show how to evaluate the integrals in the leptodermous expansion for a Woods-Saxon potential (9).

### 1. Radial action

For a potential with small surface width  $a$  the radial action can be approximately written as (see discussion of eqn. (40))

$$s_r/\hbar \approx \int_{r_{in}}^{R_0} \sqrt{E + V_0 - L^2/r^2} dr \quad (\text{A1})$$

$$+ \int_0^{r_{out}} \sqrt{E - V(r) - L^2/R_0^2} dr$$

$$- \int_0^{R_0} \sqrt{E + V_0 - L^2/R_0^2} dr.$$

The first integral is the radial action for the spherical cavity. The third integral is trivial: the integrand is a constant. Introducing  $k = \sqrt{E + V_0}$  and  $\hat{L} = L/\hbar k R_0$  to simplify the notation, it is given by  $\hbar k R_0 \sqrt{1 - \hat{L}^2}$ . The second integral is more difficult. Rewriting the Woods-Saxon potential (9) as

$$V(r) = -V_0 + \frac{V_0}{2} \left( 1 + \tanh \left( \frac{r - R_0}{2a} \right) \right) \quad (\text{A2})$$

and substituting  $y = (r - R_0)/a$ , we are led to

$$\frac{\sqrt{2}\hat{a}}{P} \int_{-1/2\hat{a}}^{\text{artanh}(c)} \sqrt{c - \tanh(y)} dy \quad (\text{A3})$$

with  $c = 2P^2(1 - \hat{L}^2) - 1$ ,  $P = \sqrt{(E + V_0)/V_0}$ , and  $\hat{a} = a/R_0$ . This expression can be evaluated analytically

$$2\hat{a} \left\{ \sqrt{1 - \hat{L}^2} \text{artanh} \sqrt{\frac{1 - \hat{L}^2 - \frac{1 + \tanh(-1/2\hat{a})}{2P^2}}{1 - \hat{L}^2}} \right. \quad (\text{A4})$$

$$\left. - \sqrt{\frac{1}{P^2} - (1 - \hat{L}^2)} \arctan \sqrt{\frac{1 - \hat{L}^2 - \frac{1 + \tanh(-1/2\hat{a})}{2P^2}}{1/P^2 - (1 - \hat{L}^2)}} \right\}.$$

Since the ansatz (eqn. (A1)) is already a first order approximation, we need only the expansion of the above expression for small  $a$ . For the second term this is straightforward

$$\arctan \sqrt{c} = \arcsin \left( P \sqrt{1 - \hat{L}^2} \right) + \mathcal{O}(\hat{a}^2). \quad (\text{A5})$$

The first term is a bit more difficult, since for  $\hat{a} \rightarrow 0$  the  $\text{artanh} \sqrt{c}$  diverges as  $1/2\hat{a}$ . We find

$$2\hat{a} \text{artanh} \sqrt{c} = 1 + 2\hat{a} \ln \left( 2P \sqrt{1 - \hat{L}^2} \right) + \mathcal{O}(\hat{a}^2). \quad (\text{A6})$$

Collecting our results we see that we can expand the radial action for a Woods-Saxon potential with surface parameter  $a$  around the radial action of the corresponding spherical cavity. The term of first order in  $a$  is given by  $\hat{I}_s(P, \hat{L}) \hat{a}$  with

$$\hat{I}_s(P, \hat{L}) = \frac{2}{P} \left( P_L \ln(2P_L) - \sqrt{1 - P_L^2} \arcsin(P_L) \right), \quad (\text{A7})$$

where we have introduced  $P_L = P \sqrt{1 - \hat{L}^2}$ .

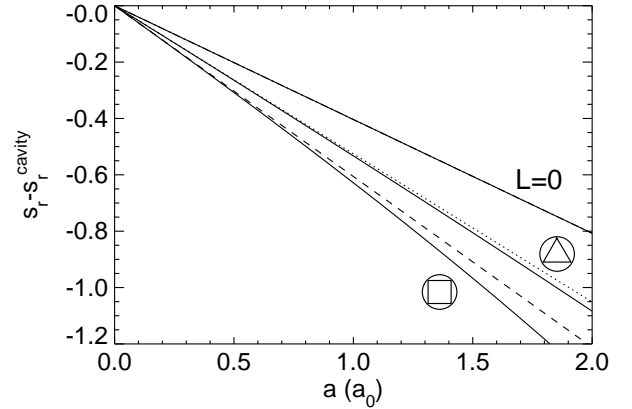


FIG. 11. Change of the radial action (in units of  $\hbar$ ) for Woods-Saxon potentials with different surface width  $a$ . The parameters for the potential are  $V_0 = 0.45 R y$  and  $R_0 = 40 a_0$ . The full lines give the radial action  $s_r(E)$  for a triangular and a square orbit.  $k = (9\pi/4)^{1/3} 1/r_s$ . The dotted line shows the change in the radial action for the triangular orbit as calculated using the leptodermous expansion ( $\hat{I}_s k a$ ). The dashed line shows the same for the square orbit.

To check how good this linearization of the radial action works in practice, we compare it to numerical results. Fig. 11 shows such a comparison for a Woods-Saxon potential that roughly resembles a sodium cluster with 1000 electrons. As can be seen, the leptodermous expansion works quite well. It is exact for  $L = 0$  (which is the quantity entering in the calculation of  $c_F$ ). For the triangular orbit the approximation is very good even for rather large surface widths  $a$ . For the square orbit the

expansion still works well, although we start to see deviations for larger  $a$ . This is due to the fact that in the leptodermous expansion we make an approximation in the angular momentum term, which becomes more critical for orbits with large  $\nu$ . It is worth noting that the change in the radial action is surprisingly linear in  $a$ . That means, we could obtain results in the spirit of the leptodermous expansion (i.e. having only phase shifts in the periodic orbit expansion), by fitting the results of numerical calculations of the action integrals with a linear function. Using such fits we could improve the accuracy of our results.

## 2. Fermi level

From equation (52) the surface term for  $\bar{k}_F r_s$  in the leptodermous expansion is given by

$$c_F = -\frac{3a}{\bar{k}_F^2} \int_0^{\bar{k}_F} \hat{I}_s(P, 0) k^2 dk. \quad (\text{A8})$$

Inserting (A7) we find

$$c_F = -\frac{6V_0^{3/2}a}{\bar{k}_F^2} \int_0^{P_F} \left[ P^2 \ln(2P) - P\sqrt{1-P^2} \arcsin(P) \right] dP, \quad (\text{A9})$$

with  $P = k/\sqrt{V_0}$ . The first integral is straightforward, the second is easily evaluated by substituting  $y = \arcsin(P)$ . We thus obtain eqn. (53) with

$$\hat{I}_N(P) = 2 \left( \ln(2P) + \left[ \frac{1}{P^2} - 1 \right]^{3/2} \arcsin(P) - \frac{1}{P^2} \right). \quad (\text{A10})$$

---

<sup>1</sup> T. P. Martin, S. Bjørnholm, J. Borggreen, C. Bréchnignac, P. Cahuzac, K. Hansen, and J. Pedersen, *Chem. Phys. Lett.* **186**, 53 (1991).

<sup>2</sup> J. Pedersen, S. Bjørnholm, J. Borggreen, K. Hansen, T. P. Martin, and H. D. Rasmussen, *Nature (London)* **353**, 733 (1991).

<sup>3</sup> C. Bréchnignac, P. Cahuzac, F. Carlier, M. de Frutos, and J. P. Roux, *Phys. Rev. B* **47**, 2271 (1993).

<sup>4</sup> M. Pellarin, B. Baguenard, C. Bordas, M. Broyer, J. Lermé, and J. L. Vialle, *Phys. Rev. B* **48**, 17645 (1993).

<sup>5</sup> H. Nishioka, K. Hansen, and B. R. Mottelson, *Phys. Rev. B* **42**, 9377 (1990).

<sup>6</sup> R. Balian and C. Bloch, *Ann. Phys. (N.Y.)* **69**, 76 (1972).

<sup>7</sup> M. C. Gutzwiller, *J. Math. Phys.* **11**, 1791 (1970).

<sup>8</sup> D. E. Beck, *Solid State Commun* **49**, 381 (1984).

<sup>9</sup> W. Ekardt, *Phys. Rev. B* **29**, 1558 (1984).

<sup>10</sup> J. Lermé, C. Bordas, M. Pellarin, B. Baguenard, J. L. Vialle, and M. Broyer, *Phys. Rev. B* **48**, 12100 (1993).

<sup>11</sup> J. Lermé, M. Pellarin, B. Baguenard, C. Bordas, J. L. Vialle, and M. Broyer, *Phys. Rev. B* **50**, 5558 (1994).

<sup>12</sup> J. Lermé, M. Pellarin, J. L. Vialle, and M. Broyer, *Phys. Rev. B* **52**, 2868 (1995).

<sup>13</sup> J. Lermé, *Phys. Rev. B* **54**, 14158 (1996)

<sup>14</sup> J. Lermé, M. Pellarin, E. Cottancin, B. Baguenard, J. L. Vialle, and M. Broyer, *Phys. Rev. B* **52**, 14163 (1995).

<sup>15</sup> E. Koch and O. Gunnarsson, *Phys. Rev. B* **54**, 5168 (1996).

<sup>16</sup> E. Koch, *Phys. Rev. Lett.* **76**, 2678 (1996).

<sup>17</sup> V. M. Strutinsky, *Nucl. Phys. A* **122**, 1 (1968).

<sup>18</sup> M. Brack, J. Damgard, A. S. Jensen, H. C. Pauli, V. M. Strutinsky, and C. Y. Wong, *Rev. Mod. Phys.* **44**, 320 (1972).

<sup>19</sup> C. Yannouleas and U. Landman, *Phys. Rev. B* **48**, 8376 (1993).

<sup>20</sup> P. Stampfli and K. H. Bennemann, *Phys. Rev. Lett.* **69**, 3471 (1992).

<sup>21</sup> G. Apai, J. F. Hamilton, J. Stohr, and A. Thompson, *Phys. Rev. Lett.* **43**, 165 (1979).

<sup>22</sup> A. Balerna, E. Bernieri, P. Picozzi, A. Reale, S. Santucci, E. Burattini, and S. Mobilio, *Surf. Sci.* **156**, 206 (1985).

<sup>23</sup> J. P. Perdew, Y. Wang, and E. Engel, *Phys. Rev. Lett.* **66**, 508 (1991).

<sup>24</sup> E. Engel and J. P. Perdew, *Phys. Rev. B* **43**, 1331 (1991).

<sup>25</sup> O. Genzken and M. Brack, *Phys. Rev. Lett.* **67**, 3286 (1991).

<sup>26</sup> M. Brack, *Rev. Mod. Phys.* **65**, 677 (1993).

<sup>27</sup> P. Hohenberg and W. Kohn, *Phys. Rev.* **136**, B864 (1964).

<sup>28</sup> W. Kohn and L. J. Sham, *Phys. Rev.* **140**, A1133 (1965).

<sup>29</sup> W. D. Knight, K. Clemenger, W. A. de Heer, W. A. Saunders, M. Y. Chou, and M. L. Cohen, *Phys. Rev. Lett.* **52**, 2141 (1984).

<sup>30</sup> K. Clemenger, *Phys. Rev. B* **44**, 12991 (1991).

<sup>31</sup> M. V. Berry and K. E. Mount, *Rep. Prog. Phys.* **35**, 315 (1972).

<sup>32</sup> M. C. Gutzwiller, *Chaos in Classical and Quantum Mechanics* (Springer, New York, 1990).

<sup>33</sup> M. Brack and R. K. Bhaduri, *Semiclassical Physics* (Addison-Wesley, Reading, 1997).

<sup>34</sup> R. P. Feynman and A. R. Hibbs, *Quantum Mechanics and Path Integrals* (McGraw-Hill, New York, 1965).

<sup>35</sup> L. S. Schulman, *Techniques and Applications of Path Integration* (Wiley, New York, 1981).

<sup>36</sup> For potentials with a very soft surface some orbits ( $\lambda, \nu$ ) may cease to exist.<sup>41,42</sup>. Since we are not concerned with such extremely soft potentials, we do not consider that case here.

<sup>37</sup> R. Balian and C. Bloch, *Ann. Phys. (N.Y.)* **60**, 401 (1970).

<sup>38</sup> Ph. J. Siemens and A. Sobiczewski, *Phys. Lett. B* **41**, 16 (1972). The equivalence of eqn. (3) with the expression given by Balian and Bloch is seen by an integration by parts.

<sup>39</sup> L. D. Landau and E. M. Lifshitz, *Quantum Mechanics* (Pergamon, New York, 1977).

<sup>40</sup> S. Flügge, *Rechenmethoden der Quantentheorie* (Springer, Heidelberg, 1990).

<sup>41</sup> J. Lermé, M. Pellarin, J. L. Vialle, B. Baguenard, and M. Broyer, *Phys. Rev. Lett.* **68**, 2818 (1992).

<sup>42</sup> J. Mansikka-aho and M. Manninen, *Phys. Rev. B* **48**, 1837 (1993).

<sup>43</sup> P. E. Lindelof, P. Hullmann, P. Bøggild, M. Persson, and S. M. Reimann, in: *Large Clusters of Atoms and Molecules*, ed. by T. P. Martin (Kluwer, Dordrecht, 1996), pp. 89.